

A COMPACT OMNIDIRECTIONAL LASER SCANNER BASED ON AN ELECTROTHERMAL TRIPOD MEMS MIRROR FOR LIDAR

Dingkang Wang, Conor Watkins, Sanjeev Koppal and Huikai Xie

Department of Electrical & Computer Engineering, University of Florida, Gainesville, FL, USA

ABSTRACT

Low-cost LiDAR with compact omnidirectional 360° scanners are needed for automobiles and robotics. This paper reports a compact omnidirectional scanner based on an electrothermal MEMS mirror, in which a circular pattern is generated by a two-axis tripod electrothermal MEMS mirror at non-resonant mode combined with a cone mirror. Meanwhile the vertical scanning field of view (FoV) up to 8° is also achieved. Compared to other omnidirectional scanners based on motorized optomechanics, this MEMS-based omnidirectional scanner has the potential to greatly decrease the size, cost and power consumption for LiDAR.

KEYWORDS:

Micromirror, Laser Scanner, Non-resonant scanning, LiDAR, Omnidirectional, Electrothermal actuator

INTRODUCTION

Low-cost, compact Light Detection and Sensing (LiDAR) sensors are the key components for autonomous driving, robotics and unmanned aerial vehicles (UAVs) [1]. 360° omnidirectional laser scanning is desired for a wide range of LiDAR applications [2]. However, most of omnidirectional scanning LiDARs are driven by motors and the vertical field of view (FoV) is typically realized by stacking multiple sets of lasers and photodetectors [3], so they are usually bulky, expensive and power-intensive [4], which greatly limits the progress of applying them in autonomous vehicles. On the other hand, MEMS scanners can scan multiple lines without moving lasers or photodetectors and are compact and low cost, but they normally cannot cover a 360° horizontal FoV [5][6].

The concept of MEMS omnidirectional scanning was previously demonstrated with a resonant biaxial electrostatic MEMS mirror [7][8]. The mirror scanned a circular pattern at resonance with a specially-designed lens module. However, this electrostatic MEMS mirror could scan a sufficiently large circular pattern only when both axes operate at resonance and both resonant modes have high Q [7]. This requires scan angle sensing and sophisticated control; even with that, it is still difficult to achieve stable scanning as the resonant frequencies, phases and Q values of those two modes are very sensitive to environmental changes and aging [9]. In addition, the device fabrication is complicated as it requires vacuum packaging that can maintain high Q for long-term use [7]. Thus, a MEMS mirror that can scan a large circular pattern at non-resonance is desired, which is exactly the focus of this work.

DESIGN OF THE MEMS MIRROR

The concept of the proposed omnidirectional scanner is shown in Figure 1(a), mainly including a laser, a 2-axis tripod electrothermally actuated MEMS mirror, and a cone

mirror. An SEM of the MEMS mirror is shown in Figure 1(b), where the mirror plate is 0.72 mm in diameter.

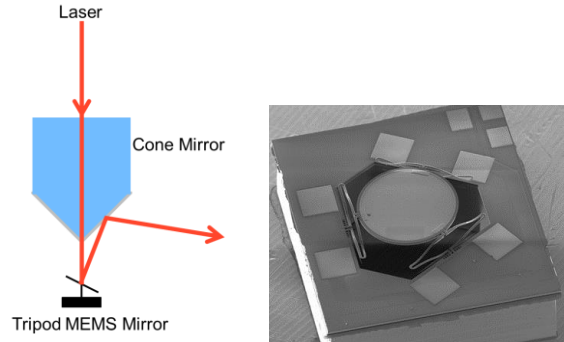


Figure 1: (a) The concept of the omnidirectional scanner. (b) The tripod MEMS mirror.

The MEMS mirror is electrothermally-actuated and based on the inverted-series-connected (ISC) bimorph actuation structure reported in [10]. By connecting two layer order-reversed bimorphs in series, as shown in Figure 2(a), both tangential tip angle θ and lateral shift (LS) are compensated. In this MEMS mirror, SiO₂ and Al are used as the two bimorph materials while Pt is used as the embedded heater material. Three groups of identical actuators are arranged around the mirror with 120° apart, forming a “tripod” configuration. The topology design of the tripod MEMS mirror is shown in Figure 2(b). Compared to the previous four-actuator designs [10] [11], this tripod MEMS mirror design simplifies the driving scheme for generating circular scanning patterns.

COMSOL is used for simulation and the simulation result is shown in Figure 3. According to the static response simulation the residual stress-induced initial displacement of the mirror plate is expected to be 170 μm above the mirror frame. The maximum displacement of the bimorph actuator is expected to be 150 μm if heated to 300 °C, which leads to a mechanical tip-tilt angle of 16° in each direction shown in Figure 3. Also, according to the modal simulation shown in Figure 4, the resonant frequencies of the piston mode and tip-tilt mode are 0.83 kHz and 1.5 kHz, respectively, assuming a 47 μm thick mirror plate is used. The 47 μm mirror plate balance balance the mirror curvature and the stiffness of the device, an SOI wafer with a device layer of 47 μm will be used for the fabrication.

DEVICE FABRICATION

The fabrication process flow is shown in Figure 5. The process is done on an SOI wafer with a device layer of 47 μm , a 1 μm -thick buried oxide (BOX) layer and a 500 μm -thick handle layer. First, a 1 μm -thick PECVD SiO₂ layer is deposited and patterned on the front side of the SOI wafer to form the bottom layer for the bimorphs containing SiO₂ as the bottom layer. Then a Cr/Pt/Cr lift-off process is

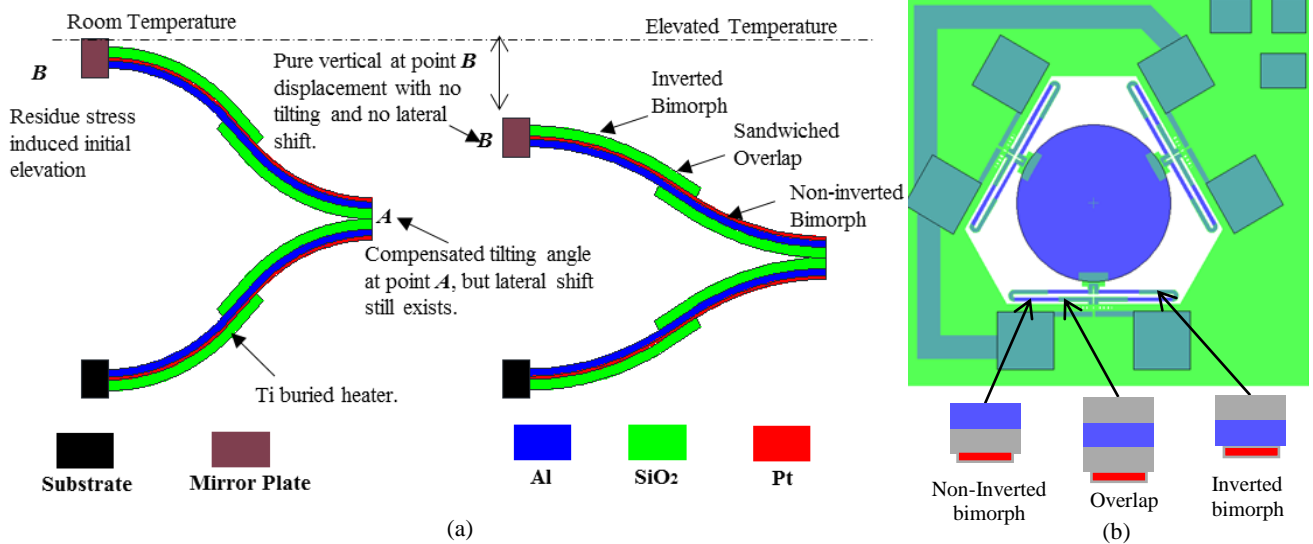


Figure 2: (a) The principle of the Invert-Series-Connected (ISC) bimorph actuator. (b) Device topology with the detailed bimorph layer configurations.

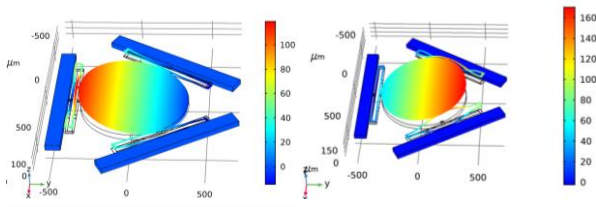


Figure 3: Simulations of static response show an mechanical scanning range of 16° with a maximum temperature of elevation of 300K.

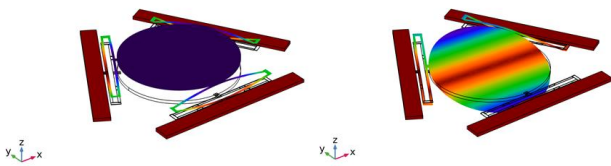


Figure 4: The simulation of resonant frequencies show the piston mode is at 830 Hz and tip-tilt mode is at 1430 Hz.

performed to form the heaters for the bimorph actuators. After that, a $0.1 \mu\text{m}$ PECVD SiO_2 layer is deposited and patterned using RIE, and then a $0.9 \mu\text{m}$ Al layer is sputtered and patterned by a lift-off process to form the other layer of the bimorph actuators as well as the electrical wiring, pads and mirror surface coating. Another $1 \mu\text{m}$ PECVD SiO_2 layer is deposited and patterned by RIE dry etch to form bimorph actuators with SiO_2 as the top layer. A silicon carrier wafer is attached to the front side of the SOI wafer for DRIE etch with a 200-nm sputtered Al_2O_3 as the mask. The DRIE etch stops at the BOX layer. Then the BOX layer is removed using RIE. After this step, the device wafer is separated from the carrier. The release starts with an anisotropic DRIE that etches through the device layer to expose the sidewalls of the silicon underneath the bimorphs. Then an isotropic etching is done to undercut the silicon blocks to release the bimorphs including both the bimorph actuators and the vertical bending bimorph array. Residual stresses in the thin films of the bimorphs result in initial out-of-plane displacement.

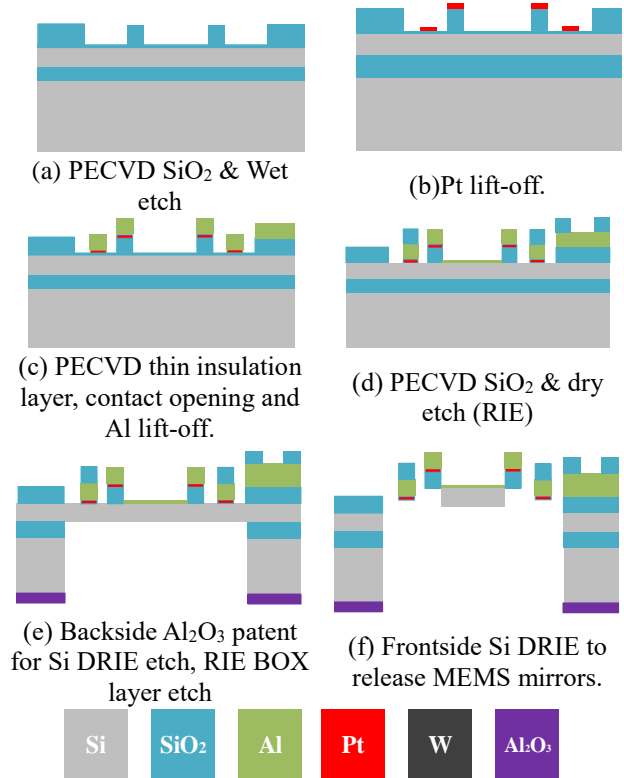


Figure 5: Fabrication process flow.

Figure 6 shows SEMs of a fabricated device, where the micromirror is suspended by three ISC electrothermal Al/ SiO_2 bimorph actuators. The initial elevation of the mirror plate shown in Figure 6 is about $195 \mu\text{m}$. The actuators form dual-S-shaped structures because of the residual stresses in the bimorph beams.

EXPERIMENT RESULT

Both quasi-static and frequency response of the tripod MEMS mirror were measured. As shown in Figure 7, the mirror had a linear optical scan angular range from 2° to 15° in all three directions under 5 Vdc. The measured

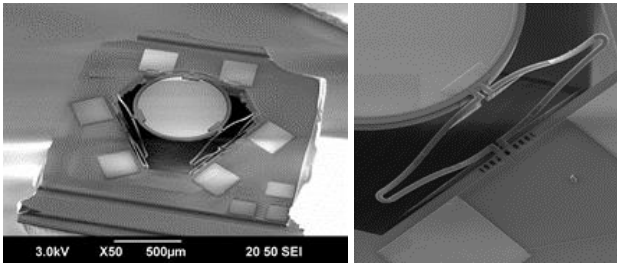


Figure 6: SEMs of a tripod MEMS mirror and a closed-up view of a bimorph actuator.

frequency response is plotted in Figure 8, showing that the 3 dB bandwidth was about 190 Hz.

Circular scan patterns were successfully obtained. In this case, three sinusoid voltage signals with the same amplitude but with a 120° phase difference from each other are applied to the three actuators respectively. Note that the circular cone angle amplitude can be tuned by changing the peak-to-peak amplitude of the sine waves. Figure 9(a) shows a circular scanning pattern of 5°, which was obtained under an amplitude of 1 V and a frequency of 30 Hz. Linearly modulating the amplitude of the driving sine signals can produce spiral patterns, which is shown in Figure 9(b). The spiral pattern can be used to achieve a vertical FoV with the cone mirror.

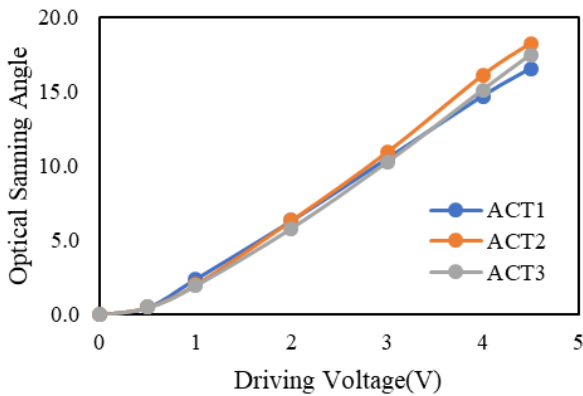


Figure 7: The static rotation angle versus applied voltage on each actuator of the micromirror.

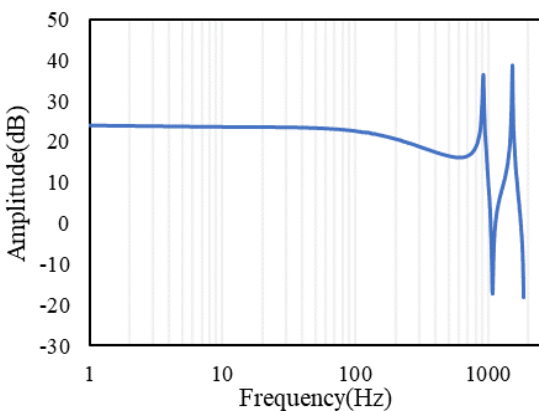


Figure 8: The frequency response of the micromirror.

The tripod MEMS mirror scans the laser on the cone mirror surface and the cone mirror reflects the laser to the horizontal direction. The experiment setup is shown in Figure 10 (a). A paper ring is placed around the scanner as the scanning target, and the scanning patterns are shown in Figures 10(b). The vertical angle of the omnidirectional mirror equals twice the mechanical tilted angle of the MEMS mirror. Through changing the amplitude of the driving signal, a vertical scanning FoV from 1° to 8° is achieved, the scanning patterns are shown in Figure 10(c).

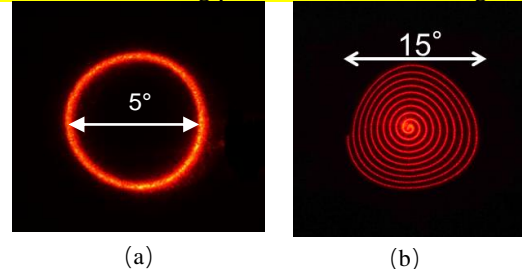


Figure 9: (a) A circular scanning pattern achieved by driving the 3 actuators with $f = 30$ Hz, $V_{offset} = 2$ V, $V_{pp} = 1$ V. (b) A spiral scanning pattern achieved at $f = 1$ Hz and scanning angle from 1° to 8°.

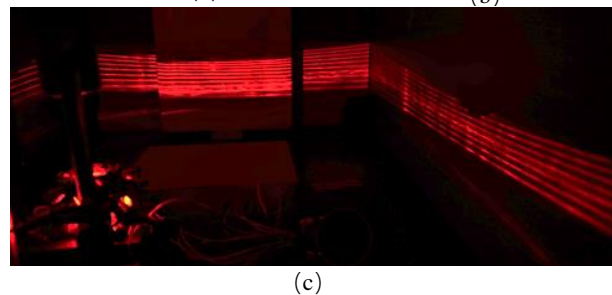
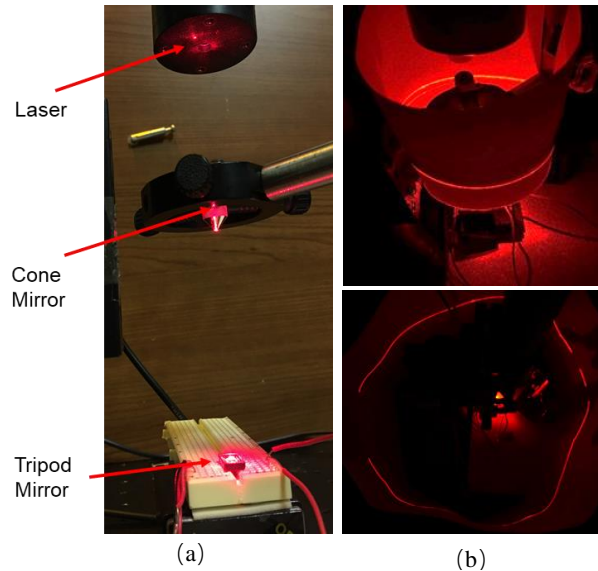


Figure 10: (a) The experiment setup of the omnidirectional scanner; (b) are achieved with a constant amplitude of driving signal which a paper ring as the target; (c) shows the vertical scanning FoV with a linearly modulated driving signal amplitude.

CONCLUSION

An omnidirectional laser scanner based on a tripod electrothermal MEMS mirror has been made. The tripod MEMS mirror can do circular scanning at a non-resonant

mode by driving the three actuators with phase-shifted driving signals. This tripod electrothermal mirror does not need complicated packaging and eliminates the issues of resonant scanning. A 45° cone mirror reflects the circular scanning pattern to the perpendicular direction to perform omnidirectional scanning. Compared to traditional motor-based omnidirectional scanners, this MEMS-based omnidirectional scanner has much smaller size, weight and power consumption. The beam divergence caused by the cone mirror is under investigation. The feasibility of applying this MEMS scanner for LiDAR will be studied in the near future.

ACKNOWLEDGEMENTS

This work is supported by the National Science Foundation under the award #1514154 and the MIST Center. Device fabrication was done at the Nanoscale Research Facility of the University of Florida.

REFERENCES

- [1] Tang, Lina; Shao, Guofan (2015-06-21). "Drone remote sensing for forestry research and practices". *Journal of Forestry Research*. 26 (4): 791–797. doi:10.1007/s11676-015-0088-y. ISSN 1007-662X.
- [2] K. Henderson, K. Stadnikia, A. Martin, A. Enqvist, S. Koppal. "Tracking Radioactive Sources through Sensor Fusion of Omnidirectional LIDAR and Isotropic Rad-Detectors" in *3D Vision (3DV), 2017 International Conference on. IEEE*, 2017, pp. 97-106.
- [3] C. Premebida, O. Ludwig, U. Nunes "LIDAR and vision-based pedestrian detection system," *Journal of Field Robotics*, 26(9), 2009, pp. 696-711.
- [4] Bruch M. Velodyne HDL-64E lidar for unmanned surface vehicle obstacle detection[J]. *Proceedings of SPIE - The International Society for Optical Engineering*, 2011, 7692:9.
- [5] S. Holmstrom, U. Baran, H. Urey. "MEMS laser scanners: a review." *Journal of Microelectromechanical Systems* 23.2, 2014, pp. 259-275.
- [6] D. Wang, S. Strassle, A. Stainsby, Y. Bai, S. Koppal, H. Xie. "A compact 3D lidar based on an electrothermal two-axis MEMS scanner for small UAV." In *Laser Radar Technology and Applications XXIII, International Society for Optics and Photonics*, Vol. 10636, 2018, pp. 106360G.
- [7] U. Hofmann, M. Aikio, J. Janes, F. Senger, V. Stenchly, J. Hagge, W. Benecke. "Resonant biaxial 7-mm MEMS mirror for omnidirectional scanning." *Journal of Micro/Nanolithography, MEMS, and MOEMS*, 13(1), 2013, pp. 011103.
- [8] Hofmann U., Janes J. "MEMS Mirror for Low Cost Laser Scanners." In: Meyer G., Valldorf J. (eds) *Advanced Microsystems for Automotive Applications 2011*. VDI-Buch. Springer, Berlin, Heidelberg
- [9] A. Hung, H. Lai, T. Lin, G. Fu, C. Lu. "An electrostatically driven 2D micro-scanning mirror with capacitive sensing for projection display." *Sensors and Actuators, A: Physical*, 222, 2014, pp. 122–129.
- [10] K. Jia, S. Pal, X. Huikai "An electrothermal tip-tilt-piston micromirror based on folded dual S-shaped bimorphs." *Journal of Microelectromechanical systems*, no. 5, 2009, pp. 1004-1015.
- [11] D. Wang, X. Zhang, L. Zhou, M. Liang, D. Zhang, H. Xie. "An ultra-fast electrothermal micromirror with bimorph actuators made of copper/tungsten." In *2017 International Conference on Optical MEMS and Nanophotonics (OMN)* (pp. 1-2). IEEE.

CONTACT

*Dingkang Wang, tel: +1-3522818843;
noplaxochia@ufl.edu